KERNFORSCHUNGSZENTRUM

KARLSRUHE

Mai 1969

KFK 1021

Institut für Angewandte Kernphysik

Experimental Gamma Ray Response Characteristics of Lithium-Drifted Germanium Detectors

W. Michaelis

GESELLSCHAFT FUR KERNFORSCHUNG M. B. H.

KARLSRUHE

NUCLEAR INSTRUMENTS AND METHODS 70 (1969) 253–261; © NORTH-HOLLAND PUBLISHING CO.

EXPERIMENTAL GAMMA RAY RESPONSE CHARACTERISTICS OF LITHIUM-DRIFTED GERMANIUM DETECTORS

W. MICHAELIS

Institut für Angewandte Kernphysik, Kernforschungszentrum Karlsruhe, Karlsruhe, Deutschland

Received 26 November 1968

This paper describes experimental determinations of absolute intrinsic efficiency, absolute total absorption probability, and peak-to-total ratio of lithium-drifted germanium diodes for gamma rays between 0.1 and 2 MeV in several detector and irradiation geometries. The sensitive volume of the crystals considered ranges from 3.8 to 28 cm^3. The results may be used as a guide in determining the optimum crystal dimensions and irradiation geometry for a given gamma-ray energy. The data are compared with simple models and, if available, with detailed theoretical calculations of the response characteristics.

1. Introduction

Since the advances of semiconductor technology have provided germanium detectors with relatively large sensitive volume increasing attention is given to the application of these devices in gamma-ray spectroscopy. While the energy resolution exceeds considerably that of conventional scintillation detectors, the photopeak efficiencies are comparatively small. Therefore detailed knowledge of the response characteristics is required in order to determine the optimum experimental conditions. Theoretical studies of the detector response have been performed using the Monte Carlo method[1,2]). Several severe problems arise in such calculations. For example, the program requires a rigorous treatment of the transport of secondary electrons produced as a result of gamma-ray interactions. The secondary electrons can leak out of the sensitive volume and therefore have a significant effect on the response. Another important problem is that of energy loss by bremsstrahlung escape. Because of these difficulties and the approximations which have to be made it is necessary to check the theoretical studies by accurate measurements. It may be recalled that even for NaI(Tl) scintillation detectors with large sensitive volumes measurements of the photofraction in most cases yielded results considerably lower than the theoretical values*. In addition, calculations of the detector response for germanium are more or less restricted to planar diodes because of the complex geometry in coaxially drifted devices. Thus extensive experimental studies are useful both for data analysis in detector applications and for a better understanding of the response characteristics.

As a contribution to this problem the present paper describes measurements of the absolute intrinsic efficiency, absolute total absorption probability and peak-to-total ratio for gamma rays between 0.1 and 2 MeV. Four detectors were used with sensitive volumes ranging from 3.8 to 28 cm^3. Each of two detectors was irradiated in two different geometries. For one diode the influence of a collimator on the basic response parameters was investigated.

2. Experimental procedure

The detector dimensions are summarized in fig. 1. Detectors 1 and 3 were true coaxial devices with two open ends. Diode 2 was a single open-ended coaxially drifted crystal. Detector 4 was a planar device with rectangular cross section. Crystals 1 and 2 were irradiated both from the frontface (closed end in case 2) with the source located on the crystal axis and from the cylindrical surface with the detector axis oriented perpendicular to the gamma-ray beam (fig. 1). Measurements with diodes 3 and 4 were performed only with the source located centrally in front of the crystals. In order to investigate the influence of a collimator on the response of detector 4 an additional run was made with this device using a lead collimator of 21 cm length and 1.0 cm internal diameter. The source was located 2.5 cm from the entrance of the collimator.

All diodes were connected to charge-sensitive preamplifiers with input stages consisting of paralleled field-effect transistors. These transistors (2N 3823) were operated at 140° K to give optimum noise performance. The energy resolution was 4.0 keV, 5.4 keV, and 3.6 keV fwhm for ^{60}Co in case of detectors 1, 2 and 3, respectively, and 2.15 keV for ^{137}Cs in case of diode 4. The operating voltage was 1000 V, 700 V, 500 V and 450 V, respectively.

The measurements were performed with a set of absolutely calibrated gamma sources†. The overall error in source strength at the reference time was ± 1%, in some cases ± 2%, the activity ranging between 5 and 21 μCi. The sources and gamma-ray energies used were ^{57}Co, 122.0 keV; ^{203}Hg, 279.2 keV; ^{22}Na, 511.0

* Ref. [3]) and the literature cited there.

† Supplied by IAEA, Division of Research and Laboratory.

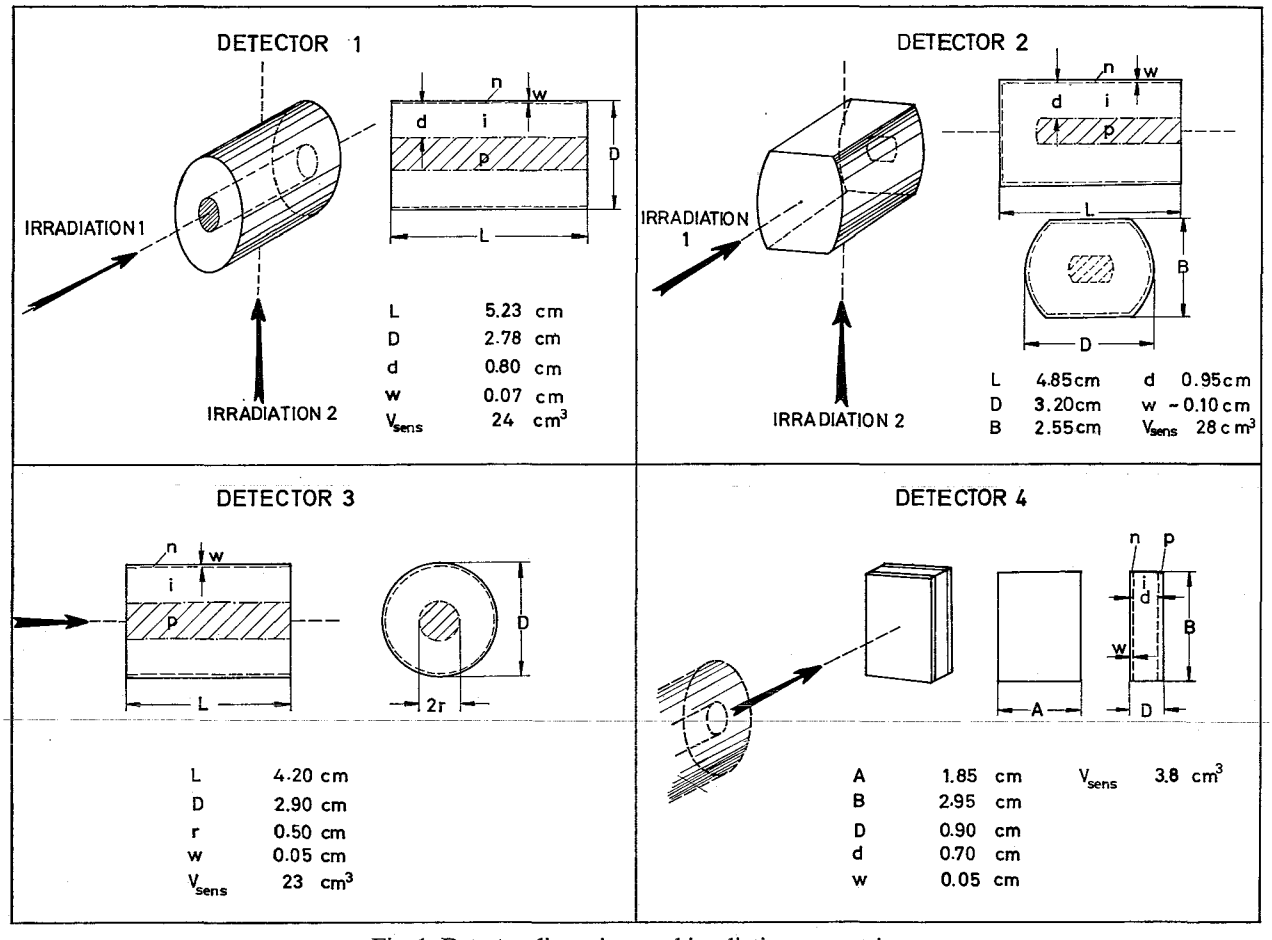

Fig. 1. Detector dimensions and irradiation geometries.

and 1274.6 keV; ^{137}Cs, 661.6 keV; ^{54}Mn, 835.0 keV; ^{60}Co, 1173.3 and 1332.5 keV; ^{88}Y, 898.0 keV and 1836.1 keV. The radioactive material was sealed between two polyethylene discs of equal thickness. The total thickness was about 0.5 mm or 35 mg/cm^2. Gamma selfabsorption in direction of the source axis could be neglected. It was about 0.3% at 60 keV and about 0.2% for 279 keV gamma rays. The ^{22}Na source was sandwiched between aluminium absorbers in order to stop all the β^+ particles. Since the source diameter was always in the order of 0.1 cm, all sources could be regarded as being point sources.

Data were accumulated by means of a 1024 channel pulse-height analyser. The spectra were carefully corrected for background.

3. Treatment of experimental data

The intrinsic efficiency is defined as the probability that the incident photon will interact and deposit at least part of its energy in the detector. The experimental spectra have to be corrected for several interfering effects. Other photons than the gamma rays considered or X-rays may be emitted by the source. In addition, photons scattered from the material surrounding the detector contribute to the counting rate. Both primary and scattered gamma rays undergo attenuation by photo-electric absorption and scattering. The following formula was used for performing appropriate corrections in a good approximation:

$$T(E) = \{(S-B)/(Q\beta\Omega\tau\,e^{-\lambda t})\}\cdot$$
$$\cdot[A(E)S(E)+(\beta'/\beta)A(E')S(E')\{T(E')/T(E)\}+$$
$$+(\gamma_K/\beta)W_K A(E_K)S(E_K)\{T(E_K)/T(E)\}+$$
$$+(\beta\Omega)^{-1}\sum_i\sum_j \beta_j\Omega_1^{(i)}f_s^{ij}\overline{\Omega_2^{(i)}}A_1(E_j)\cdot$$
$$\cdot S_1(E_j)A_2(\overline{E_s^{ij}})S_2(\overline{E_s^{ij}})\{T(\overline{E_s^{ij}})/T(E)\}]^{-1}.$$

Here

$T(E)$ = intrinsic efficiency for energy E,

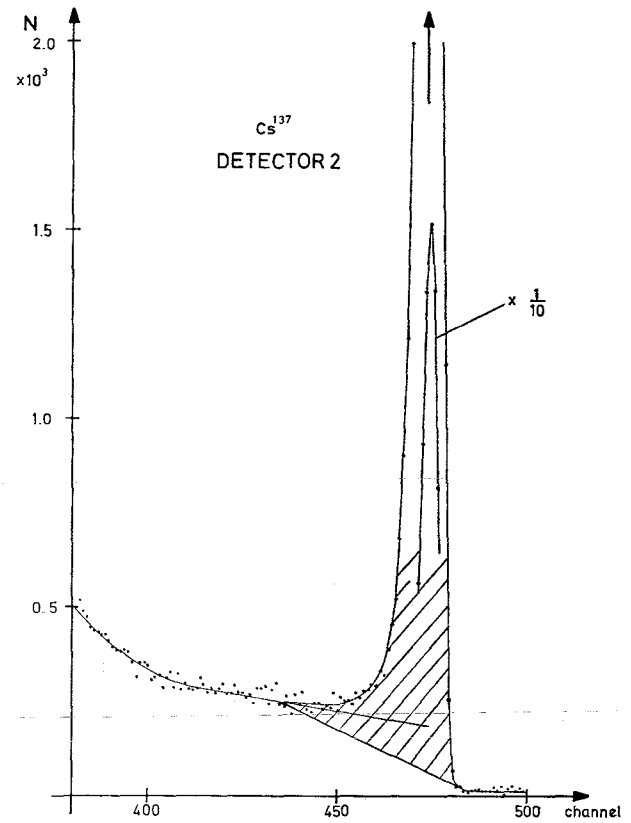

Fig. 2. Definition of peak area.

S = sum over the measured pulse-height distribution,
B = sum over the background spectrum,
Q = source strength at the reference time,
β = gamma-ray intensity per disintegration,
Ω = solid angle subtended by the detector,
τ = measuring time,
λ = decay constant of the radionuclide,
$A(E)$ = attenuation by photoelectric absorption between source and detector frontface at energy E,
$S(E)$ = attenuation by Compton scattering between source and detector frontface at energy E,
γ_K = number of K vacancies created per disintegration by K capture or internal conversion,
W_K = fluorescence yield for K X-rays,
Ω_1 = solid angle for the scattering material,
f_s = scattering probability,
$\overline{\Omega_2}$ = mean solid angle for the scattered photons,
A_1,S_1 = attenuation by photoelectric absorption and scattering between source and scattering material,
A_2,S_2 = attenuation by photoelectric absorption and scattering between scattering material and sensitive detector volume,
$\overline{E_s}$ = mean energy of scattered photons.

$\sum_i \sum_j$ denotes independent summation over all gamma rays j and scattering materials i. In the case of X-rays we have $\beta_j = \gamma_K W_K$. The prime refers to interfering gamma rays emitted by the source. The index K for E indicates K X-rays. Pulse-height distributions containing different photons of comparable intensity were unfolded using known spectrum shapes. Halflives for the decay correction were taken from [4-6]). Gamma-ray intensities per disintegration for the radionuclides used are reported in [5,7-12]). Conversion coefficients and values for the fluorescene yield were taken from [13]) and [14]), respectively. Gamma-ray attenuation coefficients of various elements are given in [15]). For the attenuation S by Compton scattering only those photons have to be considered which are scattered out of the solid angle Ω, Ω_1 or Ω_2. The influence of the angular dependence in the differential cross section can be estimated from the data given in [15]).

While Ω is clearly defined by the detector frontface area and the source-detector separation, for Ω_1 and Ω_2 which only enter into the last correction term estimated values had to be used. The determination of Ω is based on the total area of the frontface, i.e. without subtraction of the p-core and the Li diffusion.

In general, the correction terms described by the above formula were small. On the other hand, in the case of ^{203}Hg the overall correction may reach 20 or even 30%. Due to the treatment of the experimental data the results given in this paper refer to pure gamma rays of energy E and to detectors without surrounding material. Thus the data are of more general validity and independent of a special setup. Included in the results is the influence of the n-contact dead layer in case of detectors 2 and 4 since this is a property of the actual devices. The effect of the dead layer is always smaller than the experimental error above 300 keV for diode 2 and above 180 keV for diode 4.

The overall error for the intrinsic efficiency is mainly determined by the errors in the source strength, the solid angle, the spectrum unfolding and in the correction terms.

The probability that a photon striking the detector will interact and be totally absorbed is called the total absorption probability. The definition for the peak area used in the present paper is illustrated in fig. 2. This definition comprises those counts which are generally distinguished in complex gamma-ray spectra. It is based on two characteristic points in the pulse-height distribution: The first point is on the lower tail of the photopeak

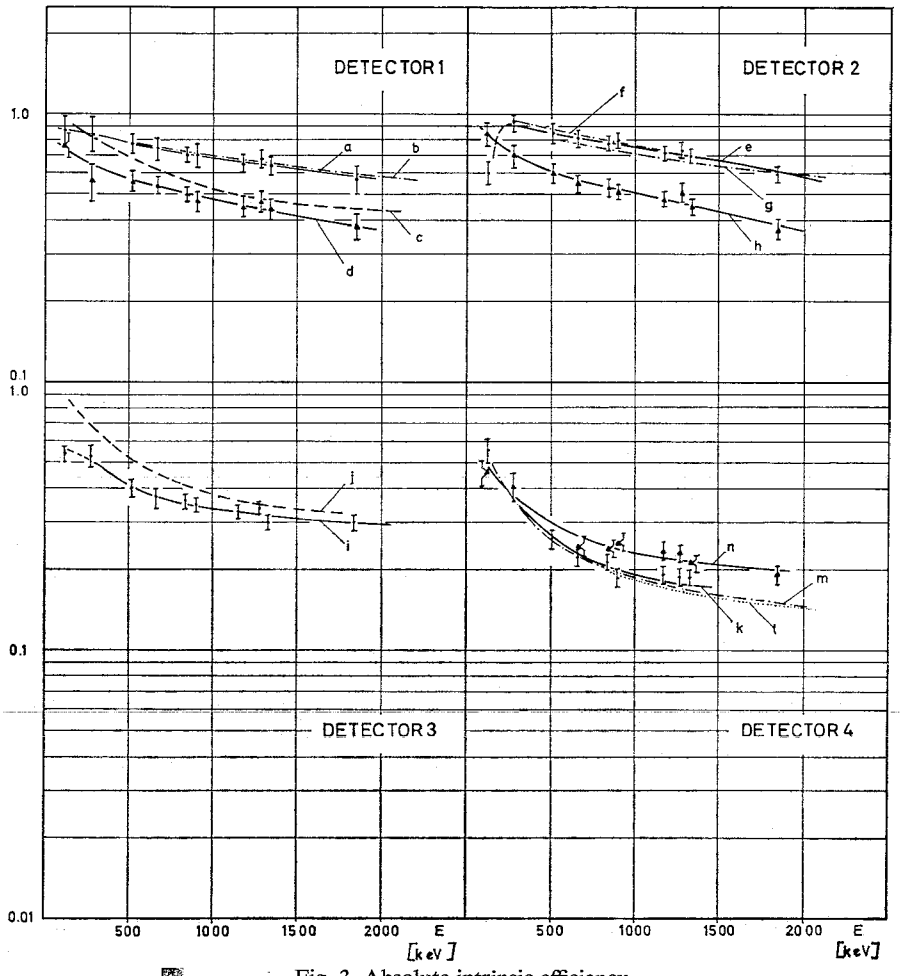

Fig. 3. Absolute intrinsic efficiency.

a. Detector 1 (24 cm³), irradiation geometry 1 (fig. 1), source-detector distance 21.6 cm;
b. Calculated from total cross section with insensitive p-core taken into account, parallel gamma-ray beam;
c. 1½″ × 2″ NaI(Tl) crystal, distance 20 cm;
d. Detector 1, irradiation geometry 2, distance 21.1 cm;
e. Detector 2 (28 cm³), irradiation geometry 1, distance 22.0 cm;
f. Calculated from total cross section without considering p-core;
g. Calculated from total cross section assuming a through p-core;
h. Detector 2, irradiation geometry 2, distance 21.0 cm;
i. Detector 3 (23 cm³), source centrally located in front of detector, distance 5.85 cm;
j. 1½″ × 2″ NaI(Tl) crystal, distance 6.0 cm;
k. Detector 4 (5.46 cm² × 0.7 cm), source centrally located in front of detector, distance 21.7 cm;
l. Theoretical curve from [1]);
m. Calculated from total cross section;
n. Detector 4, collimated gamma rays, irradiated area 1.8 cm², distance 35.7 cm.

All distance values refer to the spacing source-detector surface.

and is given by the deviation of the actual spectrum from a straight line fitted to the "background" arising from multiple Compton events. The other point occurs where the upper tail of the photopeak reaches a constant number of counts per channel. The area above the straight line connecting these points was taken as the photopeak area. The overall error for the total absorption probability is smaller than that for the intrinsic efficiency since only the errors for the source strength and the solid angle enter markedly. The error for the peak area determination can be kept small and was always $< 1\%$.

The peak-to-total ratio is defined as the ratio of the total absorption probability to the intrinsic efficiency.

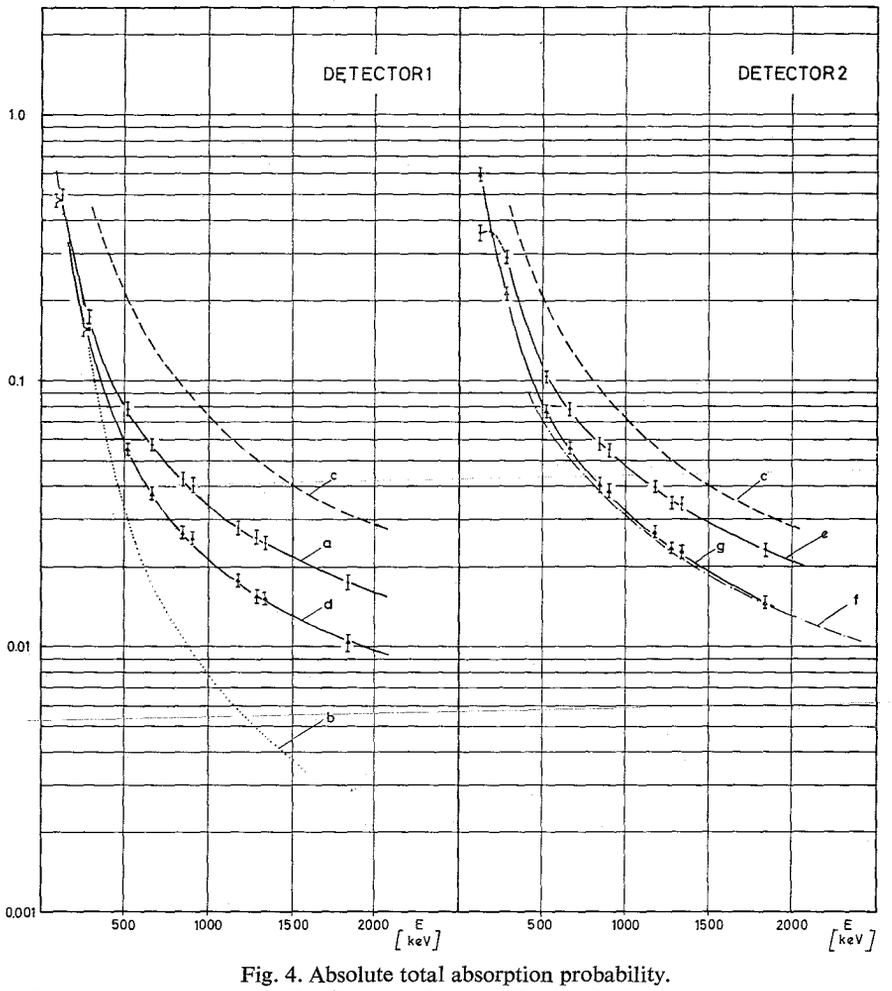

Fig. 4. Absolute total absorption probability.
a. Detector 1 (24 cm³), irradiation geometry 1 (fig. 1), source-detector distance 21.6 cm;
b. Calculated from photoelectric and total cross section with insensitive p-core taken into account, parallel gamma-ray beam;
c. $1\frac{1}{2}'' \times 1''$ NaI(Tl) crystal, distance 7 cm;
d. Detector 1, irradiation geometry 2, distance 21.1 cm;
e. Detector 2 (28 cm³), irradiation geometry 1, distance 22.0 cm;
f. Experimental curve from [20]) for a 27 cm³ detector, source centrally located in front of crystal, distance 7.6 cm;
g. Detector 2, irradiation geometry 2, distance 21.0 cm.
All distance values refer to the spacing source-detector surface.

The errors in the source strength and the solid angle do not enter into the final result.

The data given for collimated gamma radiation require a special comment. Since the effective solid angle is energy dependent and not well comprehensible the intrinsic efficiency and the total absorption probability are referred to the solid angle defined by the geometrical dimensions of the collimator exit.

4. Results

Results obtained for the absolute intrinsic efficiency are shown in fig. 3. Due to the longer distance the photons travel in the crystal in irradiation geometry 1 the efficiency is higher than that for geometry 2. The decrease at low energies for detector 2 (dashed curve) is probably caused by a thicker n-window at the front-face of the detector. For geometry 1 the intrinsic efficiency was calculated from the total cross section assuming a parallel gamma-ray beam. Attenuation coefficients for germanium were taken from [16]). Since processes which do not result in a transfer of energy to the detecting medium must be excluded contributions to the cross section due to coherent scattering have to be subtracted. For detector 1 the presence of an in-

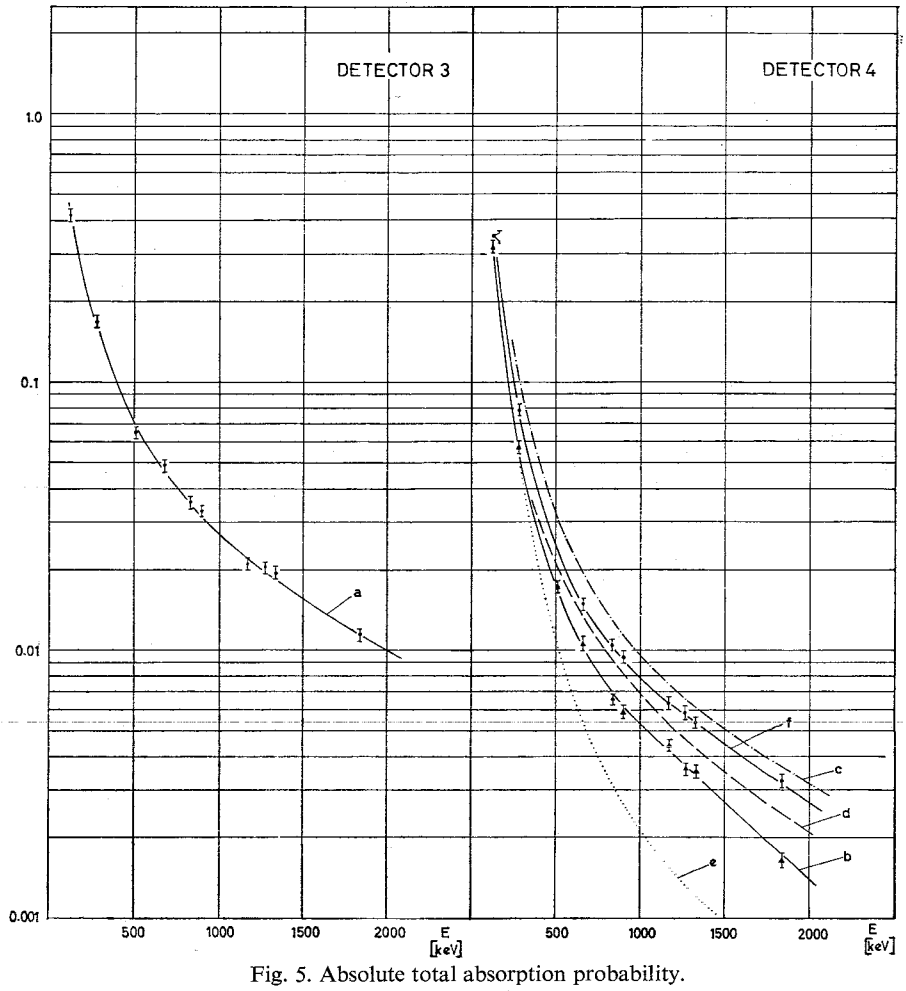

Fig. 5. Absolute total absorption probability.
a. Detector 3 (23 cm³), source centrally located in front of detector, distance 5.85 cm;
b. Detector 4 (5.46 cm² × 0.7 cm), source centrally located in front of detector, distance 21.7 cm;
c. Theoretical curve from [1]), 2.5 cm² × 0.7 cm;
d. Experimental results from [20]), 7.1 cm² × 0.7 cm;
e. Calculated from photoelectric and total cross section;
f. Detector 4, collimated gamma rays, irradiated area 1.8 cm², distance 35.7 cm.
All distance values refer to the spacing source-detector surface.

sensitive p-core was taken into account and the result of this calculation is in good agreement with the experimental data. As is to be expected from the geometry of detector 2, the experimental curve at low energies is close to the curve calculated without considering the p-core while at higher energies the experimental data are approaching the calculated results in which a through p-core has been assumed.

For comparison efficiencies for $1\frac{1}{2}'' \times 2''$ NaI(Tl) crystals have been included in fig. 3. The data were taken from [17]). In spite of the lower atomic number the intrinsic efficiency for a germanium detector of comparable size is higher than that for NaI(Tl). This is due to the lower atomic weight and the considerably higher density. On the other hand, for detector 3 (small source-detector spacing) the efficiency is lower than the curve for NaI(Tl). This inversion results from the insensitive p-core the influence of which is increasing with decreasing source-detector distance.

For detector 4 both the theoretical prediction from [1]) and the curve simply calculated from the total cross section are in good agreement with the experimental data. The intrinsic efficiency for collimated gamma rays exceeds that for uncollimated radiation at higher energies due to the energy dependence of the effective solid angle.

The results obtained for the absolute total absorption probability are summarized in figs. 4 and 5. As for the

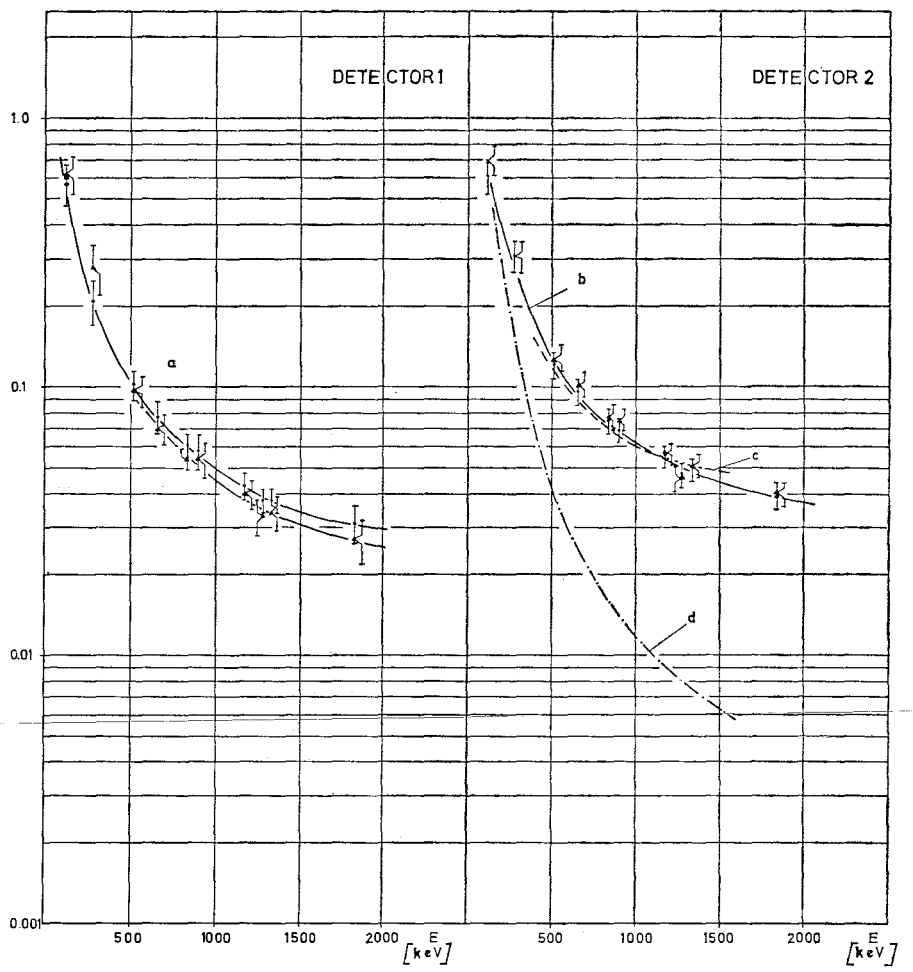

Fig. 6. Peak-to-total ratio.

a. Detector 1 (24 cm³), ● experimental points irradiation geometry 1, distance 21.6 cm, ▲ irradiation geometry 2, distance 21.1 cm;
b. Detector 2 (28 cm³), ● experimental points irradiation geometry 1, distance 22.0 cm, ▲ irradiation geometry 2, distance 21.0 cm;
c. Results from [21]) for a 30 cm³ detector;
d. Calculated from the ratio of photoelectric and total cross section.

intrinsic efficiency, the values are higher in irradiation geometry 1 than in geometry 2 due to the longer distance the photons travel in the crystal.

In two cases (detectors 1 and 4) the total absorption probability was calculated from the photoelectric and total cross section assuming a parallel gamma-ray beam. For detector 1 the p-core was taken into account. Both curves are considerably lower than the experimental results showing that, for example, in detector 1 at 1.5 MeV only about 17% of the total absorption events are due to primary photoelectric interactions. For detector 4 we obtain about 35%. Theoretically[1]) less than 20% are predicted for this fraction. A comparison of the experimental total absorption probability (fig. 5b) with the extensive theoretical treatment from [1]) (fig. 5c) for a 2.5 $cm^2 \times 0.7$ cm planar detector (interpolated from the results for thicknesses 0.1, 0.35, 0.8, and 1.2 cm) reveals a marked discrepancy at higher energies*. The above consideration on the fraction of total absorption events due to primary photoelectric interactions may lead to the conclusion that perhaps the contribution from the multiple events is overestimated theoretically. Other possible explanations may be incomplete treatment of electron leakage and bremsstrahlung escape or insufficient charge carrier collection in the diode. Rising the operating voltage, however, revealed no improvement of the peak-to-total ratio. In addition, the full-energy peak could be well approximated by a Gaussian function†. The measurements on the intrinsic efficiency

* As to the influence of the n-contact dead layer, section 3.

† I.e. small amplitudes of the correction term in the analytical line shape representation given in [18]).

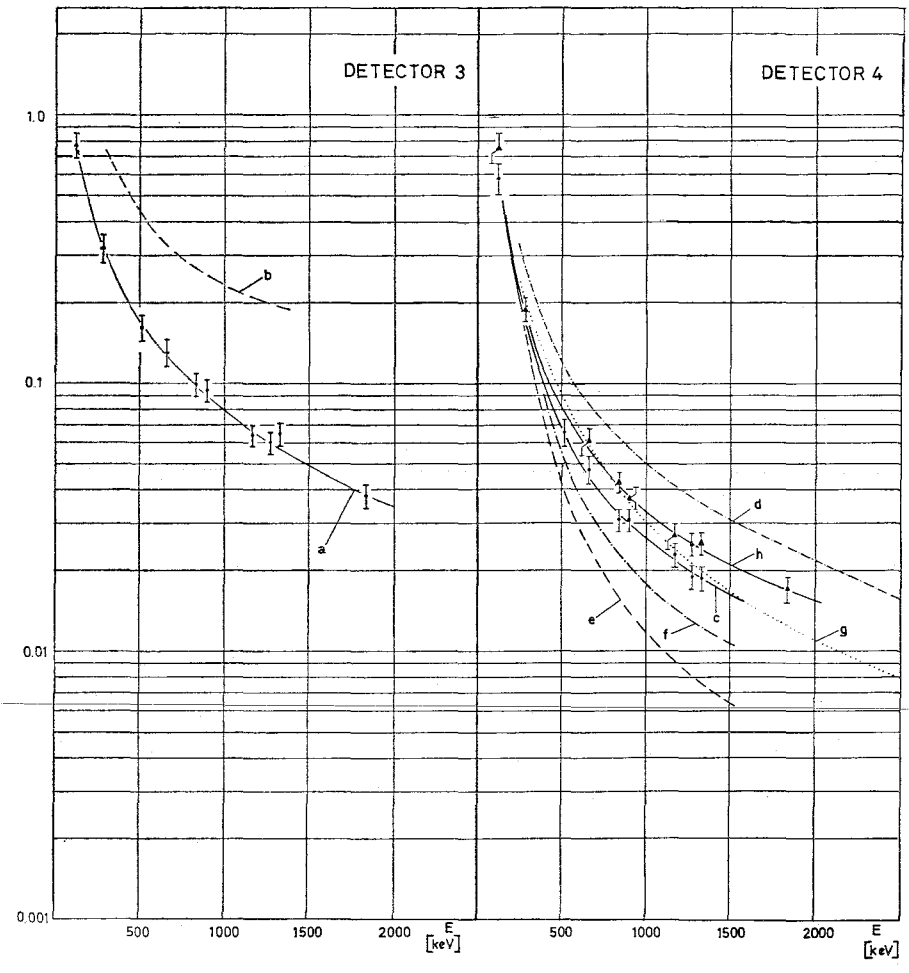

Fig. 7. Peak-to-total ratio.
a. Detector 3 (23 cm³), source centrally located in front of detector, distance 5.85 cm.
b. 1½″ × 1″ NaI(Tl) crystal, distance 2.5 cm;
c. Detector 4 (5.46 cm² × 0.7 cm), source centrally located in front of detector, distance 21.7 cm;
d. Theoretical curve from [1]) for 0.7 cm detector thickness;
e. Calculated from the ratio of photoelectric and total cross section;
f. Experimental curve from [21]) for 0.35 cm detector thickness;
g. Theoretical curve from [1]) for 0.35 cm detector thickness;
h. Detector 4 (5.46 cm² × 0.7 cm), collimated gamma rays, irradiated area 1.8 cm², distance 35.7 cm.

furthermore confirm the value of depletion depth derived from capacitance measurements. Possible effects of clean-up time on peak efficiency with constant depletion depth and resolution[19]) can hardly account for the observed discrepancy.

Disagreement between theory and experiment is also found if the empirical results reported by other authors are compared with the calculated predictions. For illustration the data from [20]) for a 7.1 cm² × 0.7 cm detector have been included in fig. 5. As is expected this curve lies somewhat higher than the present result for the 5.46 cm² × 0.7 cm diode, but again the experimental data are considerably lower than the theoretical values despite a much larger detector area. Another example is discussed below (also fig. 7).

The total absorption probability for the collimated gamma rays exceeds that for uncollimated radiation for two reasons. Firstly, as for the intrinsic efficiency the effective solid angle increases with increasing energy. On the other hand, the geometry is more favourable for multiple processes. This is seen from the improved peak-to-total ratio shown in fig. 7h.

For comparison fig. 4f gives the results reported in [20]) for another single open-ended device with a

sensitive volume of 27 cm^3. The lower total absorption probability is mainly due to the smaller source-detector spacing. That the results agree fairly well with the present data is easily seen by comparing fig. 4f with fig. 5a.

In contrast to the intrinsic efficiency the total absorption probability for germanium does not nearly reach the values for NaI(Tl) since the photoelectric cross section varies as Z^5 (fig. 4c).

The results obtained for the peak-to-total ratio are illustrated in figs. 6 and 7. Irradiation geometries 1 and 2 reveal nearly the same ratios. The difference between the curves observed is within experimental errors. Values reported in [21]) for a 30 cm^3 double open-ended coaxial diode agree very well with the present data for the 28 cm^3 device, in particular if the statement in [21]) is considered that the total includes a small contribution from gamma rays Compton scattered in the mounting material. For comparison peak-to-total ratios calculated from the ratio of photoelectric and total cross section have been included in the figures. As a consequence of the observed discrepancy between experimental and Monte Carlo values for the total absorption probability disagreement is also found for the peak-to-total in case of detector 4 (theoretical data interpolated from the values for thicknesses 0.1, 0.35, 0.8 and 1.2 cm). Similar disagreement is obtained when comparing the experimental peak-to-total ratio reported in [21]) with the theoretical prediction for a 0.35 cm thick planar diode. This provides another example for the above discussion on the experimental and calculated total absorption probabilities.

The peak-to-total ratio for the collimated beam is slightly higher than that for uncollimated radiation. The difference is somewhat smaller than expected since two effects counteract the enhancement caused by improved detector geometry. Due to the energy dependence of the effective solid angle the irradiated detector area is increasing with energy. On the other hand, gamma rays Compton scattered from the walls of the collimator contribute to the total counting rate.

Tables of the experimental data summarized in figs. 3 to 7 are presented in [22]).

The author gratefully acknowledges the help of Mr. H. Küpfer in recording the spectra and in evaluating the data.

References

1) K. M. Wainio, Thesis (University of Michigan, 1965); K. M. Wainio and C. F. Knoll, Nucl. Instr. and Meth. **44** (1966) 213.
2) N. V. de Castro Faria and R. J. A. Levesque, Nucl. Instr. and Meth. **46** (1967) 325.
3) C. Weitkamp, Nucl. Instr. and Meth. **23** (1963) 10.
4) S. C. Anspach, L. M. Cavallo, S. B. Garfinkel, J. M. R. Hutchinson and C. N. Smith, *Halflives of materials used in the preparation of standard reference materials of 19 radioactive nuclides* (National Bureau of Standards, Washington, 1966).
5) A. Artna, Nuclear Data Group ORNL (1965).
6) S. G. Gortics, W. E. Kunz and A. E. Nash, Nucleonics **21** (1963) 63.
7) R. G. Albridge and D. C. Hull, Bull. Am. Phys. Soc. **10** (1965) 244.
8) G. D. Sprouse and S. S. Hanna, Nuclear Physics **74** (1965) 177.
9) J. M. Mathiesen and J. P. Hurley, Nuclear Physics **72** (1965) 475.
10) J. G. V. Taylor, AECL PRP 49 (1961).
11) NDS 59-4-19; 61-3-56; 60-5-27; 62-3-145 (1964).
12) M. Sakai, T. Yamazaki and J. M. Hollander, Nuclear Physics **84** (1966) 302.
13) D. Strominger, J. M. Hollander and G. T. Seaborg, Rev. Mod. Phys. **30** (1958) 585.
14) C. E. Crouthamel, *Applied gamma-ray spectrometry* (Pergamon Press, 1960).
15) C. M. Davisson, in *Alpha-, beta- and gamma-ray spectroscopy* **1** (ed. K. Siegbahn; North-Holland Publishing Company, Amsterdam, 1965).
16) G. T. Chapman, Nucl. Instr. and Meth. **52** (1967) 101.
17) W. E. Mott and R. B. Sutton, in *Handbuch der Physik* **45** (ed. S. Flügge; Springer, 1958).
18) W Michaelis and H. Küpfer, Nucl. Instr. and Meth. **56** (1967) 181.
19) R. M. Green and P. P. Webb, AED-Conf. 136-003 (1967).
20) P. P. Webb, R. M. Green, I. L. Fowler and H. L. Malm, AECL-2573 (1966).
21) H. L. Malm, AECL-2550 (1966).
22) W. Michaelis, KFK 865 (1968).